Hazard-Consistent Ground Motions: Generation on the Basis of Uniform Hazard Fourier Spectra

Article *in* Bulletin of the Seismological Society of America · September 2000

DOI: 10.1785/0119990107

1 author:

Vladimir Sokolov
Saudi Geological Survey

Bulletin of the Seismological Society of America, 90, 4, pp. 1010–1027, August 2000

Hazard-Consistent Ground Motions: Generation on the Basis of Uniform Hazard Fourier Spectra

by Vladimir Y. Sokolov

Abstract Design seismic forces depend on peak ground acceleration (PGA) values and on the shape of response spectra (RS) dictated by building codes or that need to be evaluated on a site-specific basis. The PGA values and RS strictly depend on earthquake magnitude and distance, style of faulting and in cases, near-source effects (e.g., rupture directivity), as well as on the regional and local geological conditions. At present, there is no doubt that it is necessary to construct so-called site- and region-specific building code provisions reflecting the influence of different magnitude events at different distances that may occur during the lifetime of the construction, as well as the variety of local ground conditions. A scheme of Uniform Hazard Response Spectra and PGA estimation considering local site response is described in this article. The assessments of these design parameters are obtained on the basis of Uniform Hazard Fourier spectra using the concept of "dominant earthquakes". The effect of local geology is included by means of the soil/reference site spectral ratios. The results of using the method are presented for the regions characterized by different seismicity and tectonics and compared with the data obtained during the recent strong earthquakes: the Caucasus (Armenia, the 1988 Spitak earthquake region) and the Turan Plate (Central Asia, the 1979 and 1984 Gazli earthquakes region).

Introduction

Design seismic forces for buildings depend on peak ground acceleration (PGA) values and on the shape of response spectra (RS) that are dictated by building codes (see Paz, 1994, for description of the codes) or need to be evaluated on a site-specific basis. Underestimation of PGA or wrong evaluation of response spectra can lead to grave consequences during the earthquakes. Recent destructive earthquakes, including the 1985 Michoacan earthquake in Mexico (Esteva, 1988), the 1988 Spitak earthquake in Armenia (Wyllie and Filson, 1989; Yegian *et al.,* 1994a,b), the 1995 Hyogo-Ken Nanbu (Kobe) earthquake in Japan (Irikura *et al.,* 1996), the 1995 Neftegorsk (north Sakhalin) earthquake in Russia (Semenov *et al.,* 1996) and the 1999 Chi-Chi earthquake in Taiwan (Shin *et al.,* 2000) indicate the urgent necessity to revise local building code provisions, at least for the regions mentioned, because in these places the earthquakes were more severe than the provisions allowed for.

The PGA values and RS strictly depend on earthquake magnitude and distance, style of faulting and in cases, near-source effects (e.g., rupture directivity), as well as on the regional and local geological conditions. At the present, there is no doubt that instead of standard design parameters, it is necessary to construct site-specific parameters reflecting the influence from different magnitude events at different distances that may occur with a certain probability during the lifetime of the construction, as well as the variety of local site conditions. Probabilistic seismic hazard analysis (PSHA) is the efficient tool for this purpose, because it produces integrated description of the influence from all damaging events at all possible locations with respect to a specific case. It is common practice to estimate so-called uniform hazard response spectra (UHS), which represent uniform probabilities of spectral amplitude exceedance during a specified time period (EERI, 1989), and the design spectra are constructed on the basis of UHS. This approach requires a region-specific ground-motion-attenuation model that describes the relation between the ground-motion parameter (spectral amplitude at fixed frequency), earthquake magnitude, distance, and site conditions.

Several approaches have been used to include local-site effects into PSHA. One of them is based on introduction of a site coefficient to modify PGA or spectral shape (e.g., Toki *et al.,* 1991; Borcherdt, 1994). It requires the site classification depending on the geotechnical properties (shear-wave velocity, Borcherdt, 1994), or geological conditions (Toki *et al.,* 1991). Obviously, these site coefficients depend on the frequency content and intensity of the input motion and, therefore, on earthquake magnitude, distance, and regional peculiarities of the seismic-wave excitation and propagation. Campbell and Bozorgnia (1994) provided the relation between PGA "site coefficient" (ratio of the PGA on alluvium to that on a hard rock) and distance to seismogenic rupture. Borcherdt (1994) presented a methodology to estimate amplification factors for a wide range of soil types (rock description and average shear-wave velocity to a depth of 30 m) and intensity of input ground motion. However, these methods are based on the observed strong-motion amplification in San Francisco and Los Angeles regions. It has been shown by Jacob (1991) that the California-derived amplification factors should not be used in the eastern United States or Canada due to difference in the regional reference bedrock velocity. The simplified classification of a site geology is not applicable in the cases of deposits that are characterized by complex structure and configuration of bedrock surface, for example, alluvium-filled valleys and canyons.

In the second approach, the empirical attenuation relations developed for different site conditions are used. Trifunac (1990) compiled microzonation maps in terms of UHS on the basis of attenuation model, which depends on the depth of sedimentary deposits. Petersen *et al.* (1997) used different attenuation relations to calculate hazard for alluvium, soft-rock, and hard-rock site conditions. Obviously, it is not possible to obtain the attenuation functions for a variety of local soil conditions, and the aforementioned maps reveal only the gross features of the geology. In order to take into consideration site-specific amplification factor, Petersen *et al.* (1991) used the ratios between the observed response spectra and those predicted from regional attenuation relationship for rock at appropriate epicentral distances.

On the other hand, depending on the material employed and the construction of the structure, the range of the damping ratio in structural systems lies between 2% and 20% of critical damping (Newmark and Hall, 1973). The capacity spectrum method, which is used for a performance evaluation (e.g., Krawinkler, 1995; FEMA, 1999) requires both the 5% response spectra and the highly damped ones. Therefore, it is necessary to obtain a family of curves corresponding to different values of damping. As a rule, the empirical equations allow calculation of 5% damped response spectra. A stochastic model, site-response computations, and Monte Carlo statistics were used by Shapira and Van Eck (1993) to synthesize the site-specific UHS. The synthetic earthquake catalogues are created and the ground-motion time series are calculated for every earthquake on the basis of stochastic approach (Boore, 1983). The synthetic *S*-wave acceleration time histories are transmitted through the soil layer models. This approach allows to obtain the response spectra for all necessary damping values, as well as the estimations of peak acceleration, but resulted in thousands of ground-motion simulations and computations of soil-model response.

Taking into account the aforementioned problems, the probabilistic seismic-hazard analysis that is based on Fourier acceleration spectra (FAS) seems to meet the requirements of earthquake engineering practice to estimate so-called "site & region & return period-specific" strong ground motion parameters. The ground-motion input data that are crucial in PSHA are the source-scaling models, attenuation relationships, and site-response characteristics. Let us briefly discuss these models regarding the Fourier amplitude spectra, peak amplitudes, and response spectra to outline the advantages of using FAS.

Source scaling models and attenuation relations. There are two approaches to describe Fourier acceleration spectra as a function of magnitude and distance. The first one is based on statistical analysis of empirical data to estimate an equation of regression (e.g., Chernov, 1989; Trifunac and Lee, 1989; Atkinson and Mereu, 1992; Atkinson and Silva, 1997; Sokolov, 1998c). In the second approach, the Fourier amplitude spectrum is represented by a simple analytical expressions describing source, propagation, and site effect, separately. One of the widely used approaches to the prediction of ground-motion spectra is based on the so-called ω-squared point-source model (Brune, 1970). The approach revealed a good ability to describe the peak values and spectral amplitudes of ground motions in the western United States (Boore, 1983, 1987). The applicability of the ω-squared model has been tested for different seismic regions (e.g., Boore and Atkinson, 1987; Rovelli *et al.,* 1988; Mahdavian and Sasatani, 1994; Sokolov, 1998a; Sokolov *et al.,* 2000) and more complex models have been proposed (e.g., Boatwright and Choy, 1992; Atkinson, 1993). It seems to be possible to estimate the spectral model for condition of rock sites even if there is no rock reference station available (Sokolov, 1998b; Sokolov *et al.,* 2000). The finite-fault effects could be also taken into account (Beresnev and Atkinson, 1997).

When working with ground-motion peak amplitudes and response spectra, it is also possible to distinguish the same approaches as in the case of Fourier spectra. However, it is necessary to note that only the method of empirical regressions determination may be considered as a Fourier spectra independent. Much effort has recently been devoted to establishing ground-motion-attenuation relationships (see Abrahamson and Shedlock, 1997; Bommer *et al.,* 1998, for recent reviews). These empirical equations allow calculation of PGA or 5% damped response spectra for a limited set of site conditions. A large number of frequency-dependent regression coefficients should be determined. The other approach to estimate peak amplitudes and response spectra for various magnitudes and distances is based on stochastic simulation of ground-motion series (e.g., Boore and Atkinson, 1987; Atkinson and Boore, 1995, among others) and uses the models of Fourier spectra as input parameter. Therefore it should be considered as an version of the Fourier spectra-based technique.

Local site conditions. As it has been noted, the most of the recent PSHA studies were performed for the generalized soil condition or used so-called site coefficients to modify the basic values for the simplified classification of a site geology. In the case of frequency-dependent ground-motion parameters, the variety of local soil conditions may be considered using transfer (amplification) functions. Actually, it is possible to use different site transfer functions, which depend on earthquake magnitude and distance, and to consider nonlinear behavior of the soil during strong excitation. The numerous procedures of the amplification functions estimation on the basis of empirical data and numerical modeling have been developed (see Bard, 1995, for recent review, Field and Jacob, 1995 , for comparison of different techniques; Zerva *et al.,* 1999, etc.). Besides the common approach, which is based on evaluation of ratios between the spectrum on a site and a reference (rock) site, the so-called nonreference site techniques use vertical and horizontal component of the earthquake or microtremor recordings, or they employ generalized inversion schemes and utilize the data of all recorded events. The transfer functions (spectral ratios) could be applied directly to modify the Fourier amplitude spectra in order to take into account the local site effect. However, in the case of response spectra, the relation between transfer function and response spectra is not linear. For this reason, it is necessary to compute time histories of site response for several input motions using an appropriate model of soil column or to generate the site-dependent accelerograms on the basis of Fourier amplitude spectra. Of course, when working with response spectra, it is also possible to use the reference site technique. However, the choice of the reference may be very difficult: the reference site should be located on a hard-rock outcrop (or in borehole) not far from the sedimentary site, and it should provide records of almost every earthquake.

It should be noted that the term *site & region & return period-specific strong ground motion parameters* also includes seismic intensity as a useful and simple quantity describing the damage due to earthquakes. The building codes, being in force in several countries, are based on the intensity values assigned to a given seismic region (Paz, 1994), and seismic-hazard maps are often constructed to display expected intensities (e.g., Denham and Smith, 1993; Schenk *et al.,* 1996). At the same time, intensity-distribution patterns predicted for future destructive earthquake or probabilistic intensity maps are widely used for loss estimation (e.g., Shah *et al.,* 1991; Cao *et al.,* 1999). The PSHA in terms of macroseismic intensity is performed using empirical relationships between intensity, earthquake magnitude, and distance, or by converting PGA hazard maps to intensity. At present there is no doubt that seismic intensity, besides the amplitude, is an expression of the duration and frequency content of ground motion. Therefore, as it has been shown by Cao *et al.* (1999), a single peak-acceleration value may not be able to determine the loss value. In general, the adjustment of intensity values for soil condition is performed in terms of increments in macroseismic intensity. The technique which is based of the recently established relationships between intensity and the Fourier amplitude spectra (Sokolov and Chernov, 1998) allows to evaluate absolute values of intensity directly using the site-dependent spectra.

Thus, when using the Fourier amplitude spectra as a basic input in seismic-hazard analyses, it is possible to utilize a variety of the models and approaches and to choose the more appropriate ones (depending on the quality and amount of the available data) both for evaluation of the motion parameters as a function of magnitude and distance and for consideration of local site conditions. Otherwise, the choice is restricted by a limited number of attenuation relations, which were developed for a few regions and generalized site conditions, and we face before thousands of ground-motion simulations and computations of soil model response. The goal of this article is to describe a scheme that allows conversion of the uniform hazard Fourier amplitude spectra (UHFAS) to estimations of PGA, and response spectra that are used in the aseismic design practice and the building code provisions. The results of this approach and application are presented for the examples of two seismically active regions, which are characterized by different tectonics and seismicity (the Caucasus mountains, Armenia, and Central Asia, Turan plate).

Description of the Method

The method is based on Cornell's approach to probabilistic seismic-hazard assessment (Cornell, 1968), which incorporates the influence of all potential sources of earthquakes and the activity rate assigned to them. It is assumed that earthquake occurrence is a stationary random process and the time, size, and location of any earthquake are independent of the time, size, and location of every previous earthquake. However, our approach and computational scheme differ somewhat from the classical one and, therefore, it is necessary to describe the principal statements.

For a given earthquake occurrence, the probability that a ground-motion parameter X will not exceed a particular value x can be computed using the total probability theorem, that is

$$P[X \leq x] = P[X \leq x|Y]P[Y] \tag{1}$$

where Y is a vector of random variables (earthquakes of magnitude M and distance R) that influence X. Assuming that M and R are independent, the probability of nonexceedance can be written as

$$P[X \leq x] = \int\int P[X \leq x|m, r] f_M(m) f(r) dm\, dr \tag{2}$$

where $P[X \leq x \mid m, r]$ is obtained from the predictive relationship and $f_M(m)$ and $f(r)$ are the probability density functions for magnitude and distance, respectively. When performing PSHA using classical scheme, it is necessary to determine the temporal distributions of earthquake recurrence and source-to-site probability distributions for source zones. In our scheme, we do not use the probability density function $f_M(m)$ and $f(r)$, and consider every potential earthquake as a separate event. Thus, equation (1) may be rewritten as

$$P[X \leq x] = P[X \leq x|Y(m_1, r_1)] \times P[X \leq x|Y(m_2, r_2)] \times \ldots \times P[X \leq x|Y(m_N, r_N)] \quad (3)$$

where $Y(m_i, r_i)$ is the potential earthquake with magnitude $M_{min} \leq m \leq M_{max}$ and distance $R_{min} \leq r \leq R_{max}$. To characterize the source areas, a combination of so-called fault and area-source models are used. The possible earthquakes are specified by geometry (in three dimensions) and a function describing rupture area as a function of magnitude. At the same time, the earthquakes occur within the areas (source zones) that are characterized by maximum possible magnitude M_{max}. In this case, the active fault is considered as a narrow source zone rather than a line. Instead of cumulative magnitude-recurrence model that determines number N of events with a magnitude m larger than M, an alternative model is used, and N is defined as the number of events with a magnitude $m = M \pm \delta m$.

Let us assume that the level of seismic hazard is controlled by the total influence of all earthquakes that may occur in the region under study, and that the characteristics of ground motion expected during an earthquake of given M and R are lognormally distributed with standard deviation σ_x. Then, for a single earthquake of $M = m$ and focus depth $H = h$ occurred at distance $R = r$, the probability that ground-motion parameter will not exceed a given value may be estimated as follows:

$$P_{N(M=m;R=r;H=h)=1}\ [X \leq x] = \frac{1}{\sigma_x\sqrt{2\pi}} \int_{x_{min}}^{x} \exp((x - a)^2/2\sigma_x^2)dx \quad (4)$$

where a is the mean value of $\log_{10}X$ ($X -$ ground-motion characteristic) for an earthquake of given M and R; and x_{min} is of sufficiently small value ($x_{min} \approx a - 5\ \sigma_x$). Sources of ground-motion-parameter uncertainty are inherent randomness in the source rupture, the characteristics of wave-propagation path, and variability in the subsoil and geological conditions. Therefore, strictly speaking, standard deviation σ_x is a function of magnitude, distance, soil condition, and oscillator frequency (Youngs *et al.,* 1995; Somerville, 1998). Let us also assume that value a_R represents the ground-motion parameter for the reference, for example, hard rock, site. Thus, for a nonreference site, parameter a in equation (4) may be determined as $a = a_R + \Psi'$, where Ψ' is a site coefficient. If the parameter a represents the Fourier amplitude spectra at a given frequency, then the local site effect can be described by the site/reference spectra spectral ratios. In this case $a = a_R + \log_{10} \Psi$, where Ψ is the spectral amplification. To consider the uncertainty of the site response, the spectral amplification should be described as a random variable, and equation (4) may be rewritten as follows

$$P_{N(M=m;R=r;H=h)=1}\ [X \leq x] = \sum_{\Psi_{min}}^{\Psi_{max}} \left\{ \left[\frac{1}{\sigma_x\sqrt{2\pi}} \int_{x_{min}}^{x} \exp((x - a)^2/2\sigma_x^2)dx \right] * P[\Psi = \Psi_k] \right\} \quad (5)$$

where $P\ [\Psi = \Psi_k]$ is the probability that the spectral amplification equals Ψ_k. In this case it is possible to use different spectral amplification values for small and large, nearby and distant earthquakes taking into account the peculiarities of the site response that may depend on intensity of the input motion and earthquake characteristics (azimuth, earthquake depth, etc.). Most of the used techniques allow to consider the site effect only after the hazard-curve calculation, that is, the soil response is supposed to be independent on the characteristics of the earthquake source and input motion.

Equations (4) and (5) allow us to estimate the seismic effect due to a single earthquake of given characteristics (M, R, and H). If the depth of possible earthquake source may be specified only within a certain interval ($H_{min} \leq h \leq H_{max}$), then

$$P_{N(M=m;R=r)=1}\ [X \leq x] = \sum_{H_{min}}^{H_{max}} \{P_{N(M=m;R=r;H=h)=1}\ [X \leq x] * P_{M=m}[H = h]\} \quad (6)$$

where $P_{M=m}[H = h]$ is the probability that the depth (H) of the earthquake source equals h.

To consider earthquake occurrence, it is necessary to substitute the probability-distribution function for a single ($N = 1$) earthquake by the probability-distribution function for at least one ($N \geq 1$) earthquake of given M and R.

$$P_{N(M=m;R=r)\geq 1}\ [X \leq x] = \sum_{N=1}^{n} \{(P_{N(M=m;R=r)=1}\ [X \leq x])^n * P_{M=m}[N = n]\} \quad (7)$$

where $P_{M=m}[N = n]$ is the probability that n earthquakes of $M = m$ occur during specified time period t assuming a Poissonian distribution of the earthquakes. The probability is calculated as

$$P_{M=m}\ [N = n] = \frac{(\lambda_m t)^n}{n!} \exp(-\lambda_m t) \quad (8)$$

where λ_m is the average number of earthquakes of $M = m$ per unit time; n is the expected number of the earthquakes.

Considering all earthquakes of $M_{min} \leq m \leq M_{max}$ that may produce significant effect at a given distance $R = r$ and assuming their independence, we have the following

$$P_{N(R=r)\geq 1}\ [X \leq x] = \prod_{M_{\min}}^{M_{\max}} P_{N(M=m;R=r)\geq 1}\ [X \leq x] \quad (9)$$

The final expression that takes into account all distances from $R = R_{\min}$ to $R = R_{\max}$ is as follows:

$$P_{N\geq 1}\ [X \leq x] = \prod_{R=R_{\min}}^{R=R_{\max}} P_{N(R=r)\geq 1}\ [X \leq x] \quad (10)$$

Here $R_{\max}$ is the maximum distance at which the earthquake of $M = m$ may produce significant effect.

The average return period T of ground-motion parameter X exceeding the given value x may be estimated from the equation

$$P_{N=0}\ [X > x] = \exp(-\gamma_x T) = P_{N\geq 1}\ [X < x] \quad (11)$$

assuming Poissonian distribution of the events (ground-motion exceedance) with mean rate γ_x.

The technique described previously has been used for the probabilistic seismic-hazard assessment in various regions in the former USSR (the Caucasus, Central Asia, Sakhalin Island) (Chernov, 1989; Chernov and Sokolov, 1991).

To make the results of probabilistic seismic-hazard assessment clearer and more useful for engineering purposes, the so-called deaggregation procedure is used (e.g., McGuire, 1995; Bazzuro and Cornell, 1999, Harmsen *et al.,* 1999). The hazard is represented by a single or several earthquakes of certain M and R (so-called dominant earthquakes) that determine the motion in a given frequency range. Ground-motion parameters for engineering purposes can be obtained (generated or selected) for these (M, R) pairs. Generally, a single dominant earthquake will not reasonably represent the uniform-hazard spectrum, and multiple-design events should be considered. For example, McGuire (1995) proposed to study contribution to hazard for two frequencies, 1 Hz and 10 Hz, and to estimate design earthquake parameters (magnitude and distance) for short and long periods separately. Harmsen *et al.* (1999) determined dominant earthquakes for frequencies of 1 Hz and 5 Hz in the central and eastern United States and showed that the parameters of these events (M, R) depend on exceedance probability and seismicity patterns.

Since any ground-motion parameter can be extracted from the acceleration time series, in this study dominant earthquakes determined for a given return period (probability of exceedance) are used for generating ground-motion time series for the whole frequency band studied on the basis of UHFAS. These spectra are intended to provide an account for the small and large, nearby and distant events. Therefore, the time series generated on the basis of UHFAS (hazard-compatible or uniform hazard accelerograms) do not represent ground motion for a single earthquake but may be considered as a combination of the motion components in the chosen frequency band, parameters of which (spectral amplitudes) will not be exceeded with a certain probability in a specified time period (e.g., 10% in 50 years). Actually, when the engineering design requires the mutual consideration of various frequencies, say 1, 3, and 10 Hz, the vibrations at which are contributed by different events, the use of uniform hazard accelerograms for dynamic analysis could be a source of additional conservatism in engineering decisions, because it simultaneously implies the influence from several earthquakes; for example, small nearby earthquake and a large, distant one. However, in this case, standard procedure of the determination of so-called design earthquakes representing the influence of dominant (M, R) pairs may be used on the basis of the hazard deaggregation performed. The scheme of this approach is shown in Figure 1, and the details are described in the following examples. Peak ground acceleration and response spectra that are determined using these time histories are the hazard-compatible estimations.

Site Application

It is assumed that seismicity is associated with broad zones tens of kilometers wide, and the so-called area model is used. The procedure uses a system of grid points (elementary area) with 10 km × 10 km spacing. Possible earthquakes will occur within a volume of the Earth crust, and their hypocenters are located under central points of the grid. Every elementary area is characterized by the following parameters: (1) minimum ($M_{\min}$) and maximum ($M_{\max}$) magnitudes of possible earthquakes that will occur underneath the segment; (2) probability distribution of hypocentral depth for earthquake sources $M_{\min} \leq M \leq M_{\max}$; (3) rates of earthquake recurrence per unit time and unit area; and (4) source (near-field) Fourier acceleration spectra. Earthquake sources are modeled as ellipsoidal planes, and rupture area depends on the magnitude. The relationships between earth-

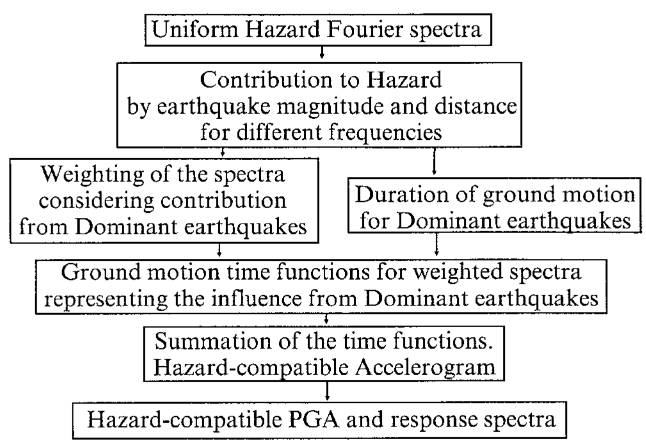

Figure 1. Scheme of probabilistic seismic hazard assessment in terms of peak ground acceleration (PGA) and response spectra on the basis of uniform hazard Fourier acceleration spectra.

quake magnitude and source dimensions proposed for reverse slip intraplate events by Shteinberg (1983) are used.

$$\log_{10} L = 0.45 M - 1.54 \quad (12)$$

$$\log_{10} S = 0.85 M \quad (13)$$

where L is the source length (km), and S is the source area (km^2). The uncertainty in the geometry of the sources is considered using the following: every source is characterized by a set of strike and dip angles (3–5 values with corresponding weights), and the distance between the site and the nearest point of the source is calculated as the average value.

Two seismic regions are considered in this study: the Turan Plate (Central Asia, Gazli region) and the Caucasus (northern Armenia, Spitak region). Catastrophic earthquakes have occurred in these regions during the last 25 years, and the observed maximum shaking intensities were more severe than the building codes provisions. The building codes used in the former USSR and, at present, in Russia (Paz, 1994) are based on the macroseismic intensity value (MSK scale) assigned to a given seismic region (so-called design intensity). Certain PGA values (design acceleration) are specified for every design intensity and, along with site-specific normalized design spectra (so-called dynamic coefficient), are used to determine lateral loads.

Gazli region. Since 1976, three major earthquakes have occurred in the Kyzyl-Kum desert of western Uzbekistan, USSR (Fig. 2). The first event on April 8, 1976 ($M_s = 7.0$) was located approximately 30 km northeast of the town of Gazli. On 17 May 1976 the second shock, with a magnitude $M_s = 7.2$, occurred approximately 20 km west of the first event. On 19 March 1984 the third large $M_s = 7.1$ earthquake occurred at a distance of approximately 20 km northwest of Gazli. All three events resulted in extensive damage to the town; observed intensities ranged from MSK VIII to MSK IX-X during the events of 1979 and MSK VIII-IX in 1984 (Djuraev *et al.,* 1986). An accelerograph installed in the epicentral area before the 17 May event recorded a maximum vertical acceleration of 1.3 g, and the maximum horizontal accelerations are about 0.6–0.7 g (Pletnev *et al.,* 1977). These earthquakes occurred in an intraplate region that had previously exhibited relatively low seismic activity. The area was assigned a low seismic risk (Medvedev, 1976), and the design intensity quoted from the building codes for the town of Gazli was MSK VII (design acceleration = 100 cm/sec^2) before 1976. However, two earthquakes with intensity VI to VII and VII to VIII were felt in the city of Bukhara, which is located 80 km SE of Gazli, in 818 and 1390 (Krestnikov *et al.,* 1980). After the earthquakes of 1976, the building code's design intensity was raised to MSK VIII (return period 1000 years; 5% probability of exceedance in 50 years; design acceleration = 200 cm/sec^2) in 1982. The schematic map of seismic source zones published after the earthquakes of 1976 (Ibragimov, 1979) is shown in Figure 2. The seismicity is associated with broad zones tens of kilometers wide that stretch along major fault zones (Bukhara and Bukhara-Ghissar). The zone boundaries are based on regional tectonic and geologic features and seismicity patterns.

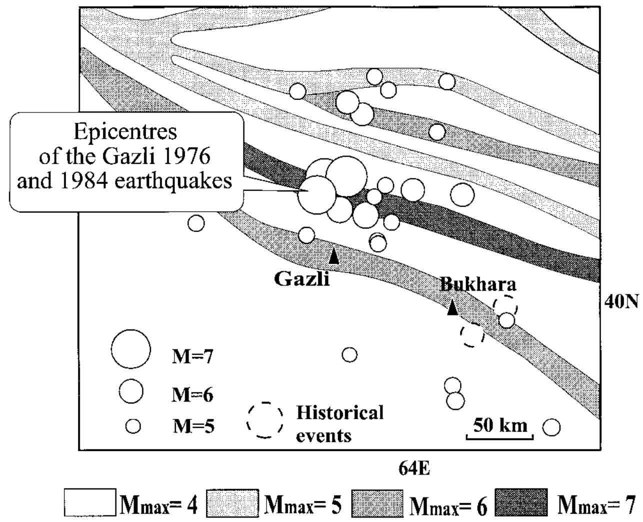

Figure 2. Schematic map of seismic source zones in the Gazli region.

Spitak region. The Spitak earthquake of 7 December 1988 (Northern Armenia, the Caucasus) caused numerous casualties and severe damage in northern Armenia (Wyllie and Filson, 1989; Yegian *et al.,* 1994a). Three main cities were affected by this earthquake: Spitak, Leninakan, and Kirovakan. Spitak experienced a devastating shock: 90% of its two-story or taller buildings either collapsed or were damaged beyond repair and were later demolished. In Leninakan the number of collapsed/demolished (two-story and taller) buildings reached 54% of total amount, and Kirovakan sustained a relatively moderate degree of damage. The design intensity stated in the building codes (1982) was MSK VIII (return period 1000 years; design acceleration = 200 cm/sec^2) for Leninakan, and MSK VII (return period 100 years, design acceleration = 100 cm/sec^2) for Spitak and Kirovakan. The maximum observed intensity (the city of Spitak) caused by the earthquake was estimated as MSK IX-X (Wyllie and Filson, 1989). Historical seismicity records show high levels of seismic activity in the region, and in 1926 a M 5.8 earthquake struck Leninakan, causing serious damage (MSK VII-VIII). In this study, the scheme of seismic source zones (Fig. 3) published in 1983 (Sikharulidze *et al.,* 1983) was used. The seismicity is associated with broad zones that stretch along major fault zones. It is supposed that large ($M > 6.0$–6.5) earthquakes may occur within the intersections of these fault zones, and the Spitak earthquake was not an exception.

It is necessary to note that for the seismic zones in Gazli and Spitak regions, M_{max} values for each zone were assigned on the basis of geological and geophysical data and historical seismicity (maximum observed historical earthquakes). Ac-

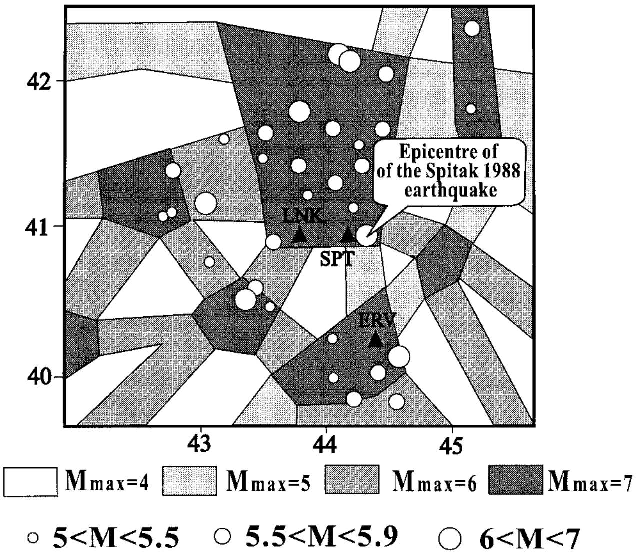

Figure 3. Schematic map of seismic source zones in the Spitak region.

tually, determination of maximum magnitudes for source zones is done subjectively, using a variety of approaches. A complex study of all available information associated with the earthquake origin (data on the geodynamics and structure of the Earth's crust, on the positions and dimensions of recently active faults, on the boundaries and sizes of individual geological blocks, on the structural depth discontinuities, as well as on the relations between geophysical fields and seismic activity) may produce detailed maps of possible maximum earthquakes varying from M 4.0–5.0 to 8.0–8.5 (e.g., Schenk *et al.,* 1996). At present, it appears also to be a general rule to assign values near 6.5–7.0 for the inactive areas, with perhaps $M_{\max}$ 7.5 to 8.0 in tectonically active fault zones (e.g., Dowrick *et al.,* 1998). However, at the same time, very low frequency of large event occurrence is assumed for the inactive areas. Using a combination of seismicity and geological data, Jakob *et al.* (1994) assigned $M_{\max}$ from M 5.5 to 7.0 to the northeastern United States (the lowest $M_{\max}$ corresponds to the lowest seismicity rate). There can be no doubt that the assessment of maximum earthquakes for source zones is ultimately a judgement involving considerable uncertainty (Coppersmith, 1991). The author intended to base the calculations, as much as possible, on the most comprehensive data (seismic-source zones and seismicity) available before the earthquakes, and only for the Gazli region the results of post-earthquake studies were used. To avoid the influence of the zone boundaries, a smoothing procedure was used: an subsidiary source zone was applied to provide a smooth change of the $M_{\max}$.

On the other hand, when basing the hazard calculation on these seismic source maps, the minimum magnitude of 4.0 should be used. It is a common practice to fix $M_{\min}$ = 5.0–5.5 because it is accepted that the smaller events could not produce a significant damage. However, the sensitivity analyses for seismic-hazard estimation showed that for short-return periods the influence of small earthquakes (M < 5) are important at high frequencies. When designing some kinds of machinery and equipment of hydrotechnical (and other) power plants, it is necessary to consider short-return periods (10–50 years) and high-frequency (up to 10–15 Hz) vibration (e.g., Masopust, 1999). It will be shown below that in the case of the Spitak region the events of M < 5 bring a certain contribution to hazard (up to 50–60%) at high frequencies (f > 8–10 Hz) and, therefore, cannot be neglected.

Earthquake recurrence models were determined for each source zone using regional catalogues on the basis of frequently used magnitude-frequency relationship

$$\log N_{\mathrm{m}} = a - bm \tag{14}$$

where a and b are the regional constants, and N_{m} is the number of earthquakes of magnitude $m \pm \delta m$ per unit time and unit area. The source spectra of ground acceleration used in calculation are shown in Figure 4. For the Spitak region, spectral scaling and attenuation models were determined on the basis of analysis of ground-motion recordings obtained in 1988–1989 during the Spitak earthquake observation (Sokolov, 1998a). The basic ω-squared Brune spectrum can be used in the Spitak region to describe ground-motion-acceleration spectra A at frequency f on rock sites in the following way (Boore, 1983)

$$A(f) = (2\pi f)^2 \, CS(f)D(R, f) \tag{15}$$

where C is the scaling factor; $S(f)$ is the source spectrum; and $D(R, f)$ is the function that accounts for the frequency-dependent attenuation.

The scaling factor is given by

$$C = (\langle R_{\theta\phi}\rangle FV)/(4\pi\rho\beta^3 \, R) \tag{16}$$

where $\langle R_{0\varphi}\rangle$ is the radiation coefficient, F is the free-surface amplification, V represents the partitions of the vector into horizontal components, ρ and β are the density and shear velocity in the source region, respectively, and R is the hypocentral distance.

A commonly used source function $S(f)$ in the Brune's (1970) model is

$$S(f) = M_0/[1 + (f/f_0)^2] \tag{17}$$

For the Brune's model, the source-acceleration spectrum at low frequencies increases as f^2 approaches a value determined by f_0 (corner frequency) and M_0 at frequencies $f \gg f_0$. The value of f_0 can be found from the relation $f_0 = 4.9 \times 10^6 \, \beta \, (\Delta\sigma/M_0)^{1/3}$. Here $\Delta\sigma$ is the stress parameter in bars, M_0 is the seismic moment in dyne-cm, and β is in km/sec. The level of the spectrum remains approximately constant for frequencies above f_0 until the cut-off frequency $f_{\max}$

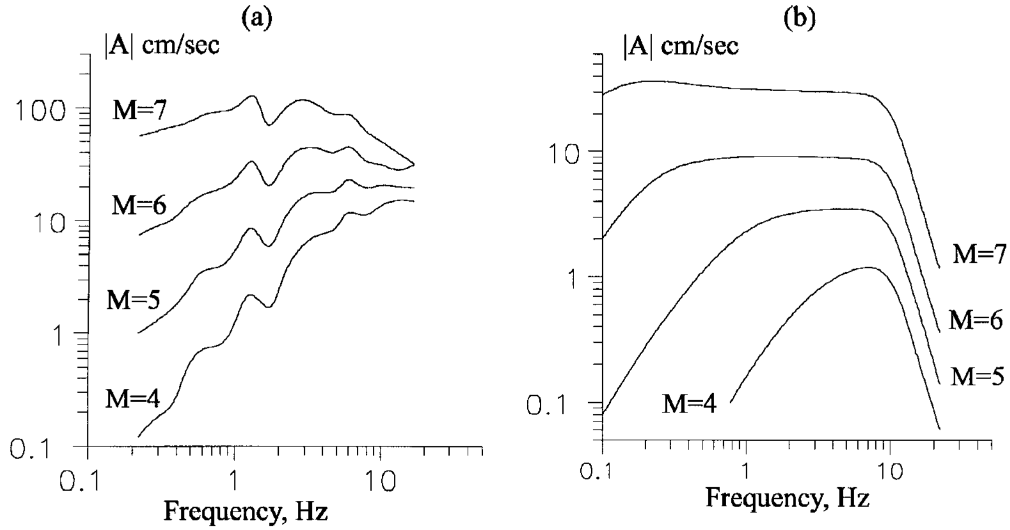

Figure 4. Source (near-field) Fourier spectra of ground acceleration. (a) the Gazli region, the empirical model based on ground motion data, soft soil; (b) The Spitak region, hard rock, Brune's ω-squared spectra.

is approached. The amplitude of the spectrum decays rapidly at frequencies above f_{max}. The function $D(R, f)$ modifies the spectral shape and depends on the hypocentral distance (R), regional crustal material properties, the frequency-dependent regional quality factor Q, and f_{max}. These effects are represented by the equation

$$D(R, f) = \exp[-\pi f R / Q(f)\beta] P(f, f_{max}) \tag{18}$$

where $P(f, f_{max})$ is a high-cut filter. For the filter the following expression (Boore, 1983) was used: $P(f, f_{max}) = [1 + (f, f_{max})^8]^{-0.5}$. The quality factor $Q(f)$ in equation (18) is determined following the empirically derived form (Boore, 1987)

$$Q = 29.4 \, [1 + (f/0.3)^{2.9}/(f/0.3)^2] \tag{19}$$

The stress-drop parameter $\Delta\sigma$ changes from 150 bars for earthquakes of $M = 4$ to 50 bars for events of $M = 7$ (Sokolov, 1998a). The values of cut-off frequency f_{max} are 10 Hz for all cases.

The empirical models of source (near-field) spectra and attenuation relations were used in the case of the Gazli region. The specific approach to the determination of empirical relationships between Fourier amplitude spectra, magnitude, and distance was developed by Chernov (1989). According to empirical data, the spectral amplitudes (A) insignificantly vary with distance near earthquake source (the so-called near-field zone). The dimensions of this zone (R_0) depend on the earthquake magnitude and are close to the source length L for moderate and strong magnitudes. Shteinberg (1986) offered to approximate R_0 by the relation

$$\log_{10} R_0 = 0.195 \text{ M} + 0.039 \tag{20}$$

A similar relation was obtained by Chernov (1989). In the far-field zone ($R > R_0$), the values $\log_{10} A$ decrease proportionally to distance, and the relationship between A and R may be represented as

$$\log_{10} A = a_0 + a_1 \log_{10} R \tag{21}$$

or

$$\log_{10} A = \log_{10} A_0 + a_1 \log_{10} (R/R_0) \tag{22}$$

where A_0 is the spectrum in the near-field zone. Coefficients a_1 determine the attenuation of the spectral amplitudes with distance and depend on the frequency f as

$$a_1 = \begin{cases} \text{const} = b + b_1 \log_{10} f_0 & \text{at } f \leq f_0 \\ b + b_1 \log_{10} f & \text{at } f > f_0 \end{cases} \tag{23}$$

Here f_0 is Brune's corner frequency.

Chernov (1989) obtained the following frequency dependence (world-mean data)

$$a_1 = (-0.68 \pm 0.08) \log_{10} f - 1.60 \pm 0.18 \tag{24}$$

The coefficients a_1 are region-dependent. In areas of relatively consolidated crust (such as the Gazli region), spectral amplitudes decrease more slowly with distance, by 20–30%, than in areas with inhomogeneous crust (for example, the Caucasus). Moreover, at distances of 50–200 km, the spectral amplitudes attenuate more slowly than at shorter distances. These results are confirmed experimentally (Trifunac and Lee, 1989; Atkinson and Mereu, 1992) and may be interpreted in terms of superimposed direct waves and waves reflected from interfaces in the middle mantle and the Moho-discontinuity.

The magnitude dependence of the Fourier spectral amplitudes are described in terms of the parameter $\beta_M = \Delta\log_{10}A/\Delta M$ (logarithmic increment of the spectral amplitudes per unit magnitude). The coefficients β_M increases with decreasing frequency; that is, as the source energy increases, the intensity of low-frequency vibrations increases more rapidly than that of high-frequency vibrations. The relation $\beta_M(f)$ can be represented as

$$\beta_M = \begin{cases} \text{const} = c + c_1 \log_{10} f_0 & \text{at } f \le f_0 \\ c + c_1 \log_{10} f & \text{at } f > f_0 \end{cases} \tag{25}$$

The parameters of relation (c and c_1) depend on the style of faulting, and for a group of reversed-fault (thrust) earthquakes, including the Gazli events of 1976 and 1984, the following averaged relation can be used (Chernov, 1989)

$$\beta_M = -0.46 \log_{10} f + 0.64 \tag{26}$$

Note that this approach accounts for both the focal mechanism effect and the regional features of the seismic radiation propagation related of geological structure. The spectral model for the Gazli region was determined on the basis of available ground-motion data obtained during the earthquakes of 1976 and 1984 (Chernov, 1989), and the spectra correspond to the following site conditions: sandy loam over stiff clay, soft soil layer thickness $\approx$ 50 m, S-wave velocity 0.3–0.4 km/sec.

Results and Discussion

It can be seen from equations (9) and (10) that the total probability of ground-motion parameter X not to be exceeded is determined by multiplication of probability functions for different M and R values. Therefore, it is possible to determine the influence from every (M, R) pair, and the "dominant earthquake" for a given return period should be characterized by the largest value $(1 - P_{(M=m;\ R=r)}\ [X \le x])$. Note that the distribution of the earthquake depths and occurrence of the events have been already taken into consideration. The value x controlling the contribution of (M, R) pairs is determined using equation (11) for a given return period T (probability of exceedance in a specified exposure time). Here R is the distance from the site to the center of the elementary area, which is considered as the "epicenter" for all earthquakes occurring at different depths underneath the area.

As a rule, a 10% probability of exceedance in 50 years applies to most building codes for ordinary buildings. It corresponds to 1/475 annual probability of exceedance (or return period of 475 years). For buildings classified within other categories of importance, the different return periods (annual probability of exceedance) may be applied (from 200 up to 2500 years). Reference return periods from about 100 to 1000 years are generally applicable to electrical system components, and larger return periods (up to 10000 years) are applicable to dams (Little and Meidal, 1994), nuclear power plants, and other critical facilities. Several building codes specify two levels of demand on structural behavior: so-called serviceability limit state (SLS) and ultimate limit state (ULS). For example, the New Zealand's code operates with SLS corresponding to return period of 20 years and ULS corresponding to return period of 1000 years, and return periods of 475 and 2500 years are used in China (Paz, 1994). The models of "cumulative damage" also require assessments for short-return periods. At the same time, short-return periods (less than 50 years) may also be useful for estimation of the hazard assessment reliability by comparing with available ground motion recordings. Therefore, in this study, various return periods (from 50 to 5000 years) have been considered.

Figures 5 and 6 show the relative contribution to Fourier spectra hazard by earthquakes of M and R for various return periods at different frequencies. For the town of Spitak (Fig. 5), the hazard for small return period ($T = 50$ years, 40% probability of exceedance in 50 years) is determined by nearby earthquakes $M = 5$ for intermediate and high frequencies ($f > 1$–2 Hz). The $M = 4$ events also bring a certain contribution (up to 50–60%) at high frequencies ($f > 8$–10 Hz) and, therefore, cannot be neglected. The nearby earthquakes of $M = 6$ are "dominant" for frequencies $f <$ 1.0–0.5 Hz, and large ($M = 7$) distant ($R > 80$–100 km) events are "dominant" in the low-frequency domain ($f < 0.3$ Hz). Distances of more than 80–100 km correspond to zones with $M_{max} = 7.0$ situated around Spitak (see Fig. 3), and bearing in mind the total area of the zones, the probability that at least one strong earthquake will occur in these zones during the time period of $T = 50$ years is considerable, as compared with the strong earthquake occurrence in the nearest area of $M_{max} = 7.0$. When increasing return period T, the influence from intermediate and large earthquakes becomes "dominant" for the whole frequency range, and the hazard is completely determined by nearby events of $M =$ 6–7 for $T > 2000$ years.

In the case of the town of Gazli (Fig. 6), the hazard is determined by nearby ($R \le 10$ km) earthquakes of $M = 6$ that may occur in the nearest seismic zone of $M_{max} = 6.0$, and by relatively distant ($R \approx 40$–60 km) earthquakes of $M = 7$ that may occur in the seismic zone of $M_{max} = 7.0$, situated north the town. It is necessary to note that the "contribution" of nearby $M = 6.0$ events increases with increasing return period, and such events are completely "dominant" for frequencies $f > 3.0$–4.0 Hz for large return periods ($T \ge 500$–1000 years). This distribution of "dominant earthquake" parameters versus return period differs from the case of the Spitak town due to peculiarities of seismic zone boundaries and location relative to the site.

To describe the procedure of the UHA generation, let us consider return period of 50 years and the Spitak area. In

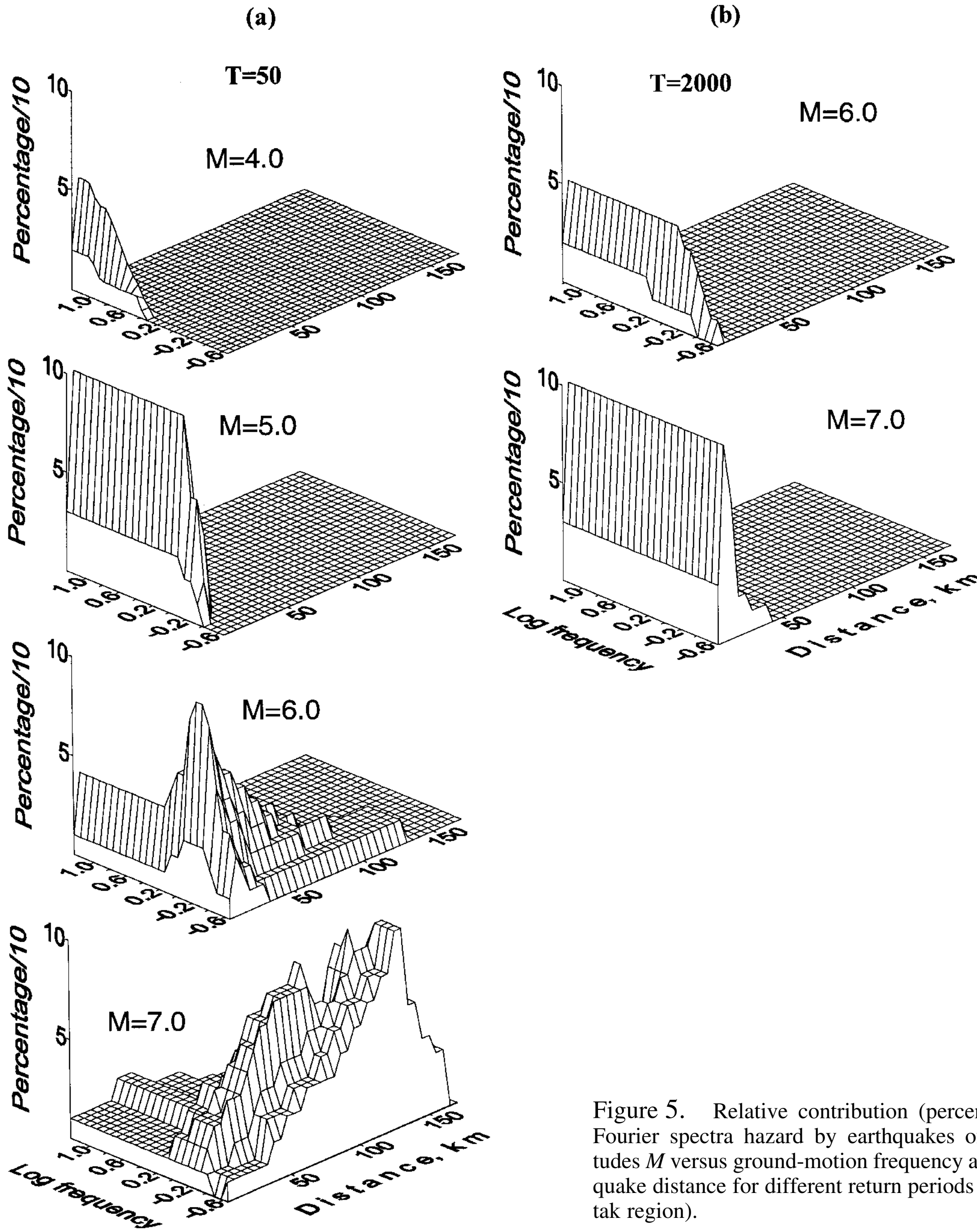

Figure 5. Relative contribution (percentage) to Fourier spectra hazard by earthquakes of magnitudes M versus ground-motion frequency and earthquake distance for different return periods (the Spitak region).

this case, bearing in mind the contribution to hazard (Fig. 5a), it is possible to choose a set of at least five "dominant earthquakes", namely: (a) $M = 4.0$, $R = 5–10$ km; (b) $M = 5.0$, $R = 5–10$ km; (c) $M = 6.0$, $R = 5–10$ km; (d) $M = 7.0$, $R = 100–120$ km, and (e) $M = 7.0$, $R = 140–150$ km. Figure 7 (solid line) shows Uniform Hazard Fourier spectrum of ground acceleration (rock site) calculated for return period of 50 years. This spectrum has been weighted taking into account the relative contribution from "dominant earthquakes" to produce "characteristic" spectra that represent influence from "dominant earthquakes" (Fig. 7, dotted lines). These spectra are used to generate the "dominant earthquake compatible" ground-motion time series. The stochastic technique proposed by Boore (1983) was applied in this study. One of the most important parameters of the technique is the duration model, in which it is assumed that most (90%) of the spectral energy is spread over a duration $\tau_{0.9}$ of the accelerogram. The frequently used duration models are the following:

$$\tau_{0.9} = \tau_0 + bR \tag{27}$$

where τ_0 is the source duration and bR represents a distant-dependent factor to account for dispersion (Atkinson, 1993; Atkinson and Boore, 1995);

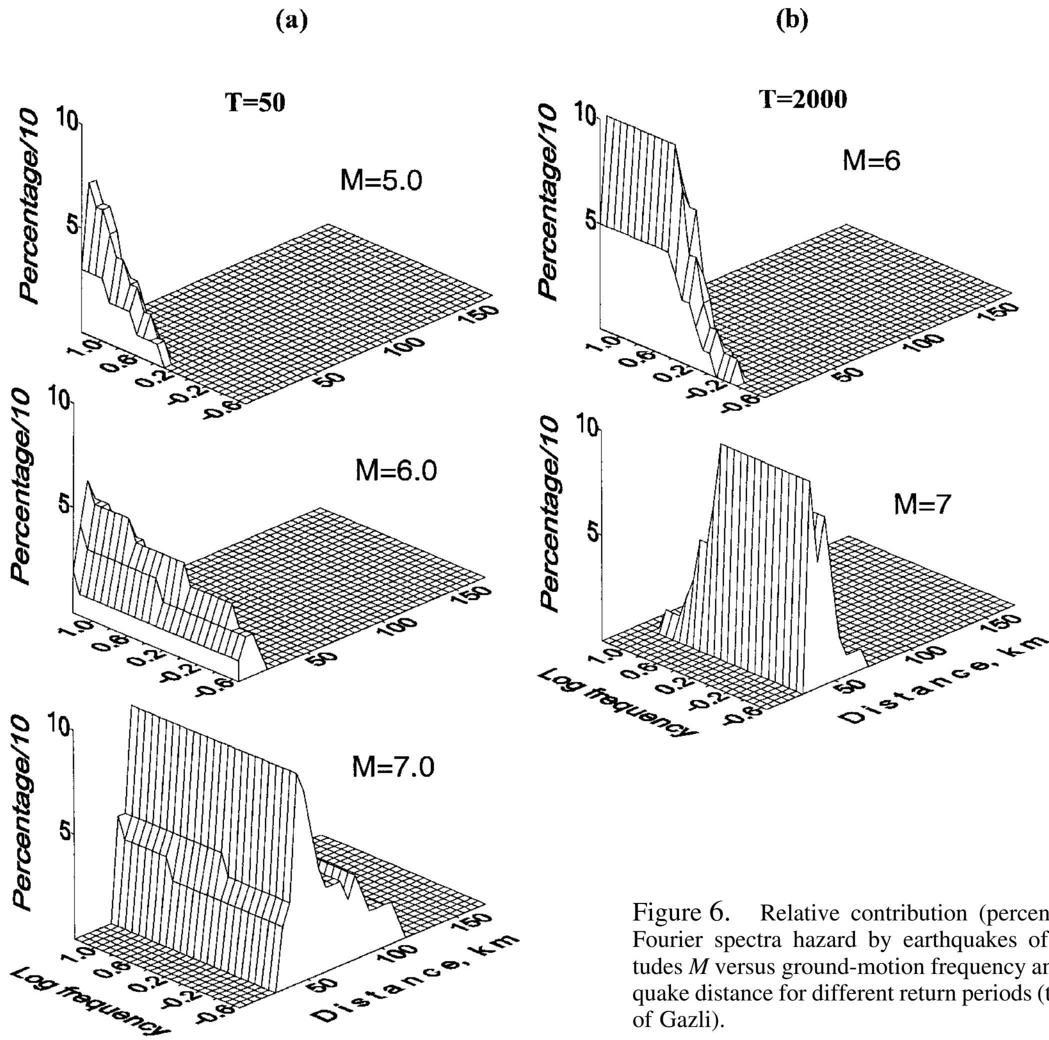

Figure 6. Relative contribution (percentage) to Fourier spectra hazard by earthquakes of magnitudes M versus ground-motion frequency and earthquake distance for different return periods (the town of Gazli).

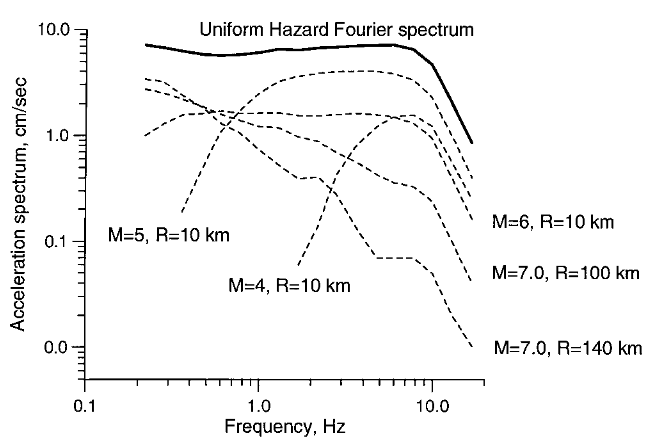

Figure 7. Uniform hazard Fourier spectrum (thick solid line) of ground acceleration (the Spitak region, hard rock, return period of 50 years) and "weighted" spectra (dashed lines) representing contribution from the "dominant earthquakes" of magnitude M and distance R.

$$\log_{10}\tau_{0.9} = 0.207\ M_S + 0.264\ \log_{10}R - 0.65 \pm 0.19 \quad (28)$$

for rock sites, and

$$\log_{10}\tau_{0.9} = 0.178\ M_S + 0.4\ \log_{10}R - 0.48 \pm 0.24 \quad (29)$$

for soft-soil sites (Shteinberg, 1986). Here R is the hypocentral distance in km.

When calculating ground-motion time series on the basis of weighted UHFAS, the duration models for rock and soil sites (equations 28–29) were used for the Spitak region, and that for soil sites (equation 29) was used for the Gazli region. A set of acceleration time functions (30–40 accelerograms) is calculated for every "characteristic spectrum" using a simple envelope function (Boore, 1983)

$$w(t) = at^b \exp(-ct)H(t) \quad (30)$$

where $H(t)$ is the unit-step function; b and c are the shape parameters. The peak of the envelope occurs at some fraction ε of a specified duration $\tau_{0.9}$, and values of b and c are determined by ε ($\varepsilon = 0.2$ in this study) and $\tau_{0.9}$ (Boore, 1983). Actually, other region- and site-dependent envelope models can be used (see, for example, Huo and Hu, 1994), and it seems to be useful to consider frequency-dependent strong-motion duration (Caillot and Bard, 1992; Trifunac and Novikova, 1995).

Figure 8a shows examples of synthetic time histories that correspond to the weighted spectra shown in Figure 7. Summation of these functions produces the uniform hazard Fourier spectrum-compatible accelerograms (UHA). Due to incoherence of summation, the summed amplitude should be multiplied by $N^{1/2}$ (Joyner and Boore, 1986; Beresnev and Atkinson, 1997) for high frequencies, where N is the number of the "characteristic accelerogram" (or "dominant earthquakes"). Figure 8b compares averaged and smoothed

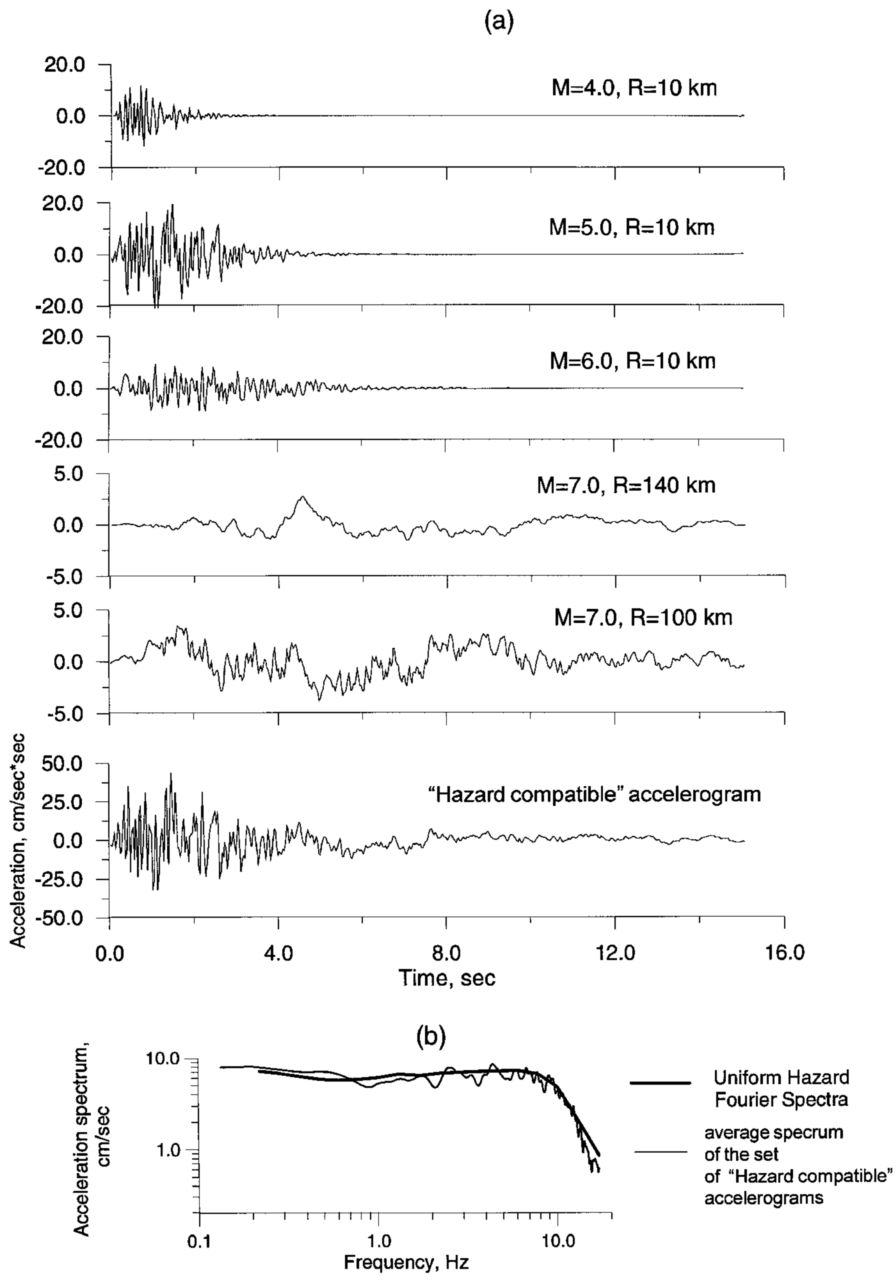

Figure 8. (a) Ground motion time functions (acceleration, cm/sec^2) representing influence from the "dominant earthquakes" (the Spitak region, hard rock, return period of 50 years) and uniform hazard accelerogram; (b) Comparison of uniform hazard Fourier spectrum (the Spitak region, hard rock, return period of 50 years) and the smoothed spectrum averaged from a set of 40 uniform hazard accelerograms.

spectrum of a set of UHAs with target uniform hazard Fourier spectrum and shows that the two match reasonably well for all frequencies. When a set of site & region & return period—dependent UHAs is calculated, the maximum amplitude averaged from the set produces the so-called PGA hazard, and the uniform hazard response spectra (UHS) can be evaluated for the necessary damping ratio. Table 1 lists PGA values estimated using this approach for different return periods and site conditions.

As previously noted, the influence of local soil condition can be accounted for using site amplification functions when estimating ground-motion parameter (Fourier spectrum at given frequency, equation 5). These amplification functions (or spectral ratios) may be different for small and large, distant and close earthquakes, reflecting nonlinear soil response. It is possible also to consider uncertainty of site response describing the latter as a random variable and introducing a probability distribution function for every frequency. "Site-dependent" UNFAS reflect occurrence of large and close events which can produce non-linear effects, and therefore UHAs should provide an account of these phenomena. In this case, however, it is necessary to describe quantitatively nonlinear behavior of site response in terms of site amplification functions. In this article the possibility of nonlinear phenomena in soil during considered events has not been taken into account.

Let us consider soil amplification effect for the city of Leninakan (at present renamed Gumri) that suffered severe damage during the Spitak earthquake (Wyllie and Filson, 1989; Yegian *et al.*, 1994a,b). The city is located in the center of a flat wide valley (20 km by 16 km). The soil deposits in this basin consist of a top 35–50 m of stiff silty-sandy clays, occasionally containing layers of sand and tuff, underlain by about 300–350 m of very stiff lacustrine clays. Figure 9a shows the spectral amplification function (*SV*-waves, soil/rock) for Leninakan calculated using soil model data published in Wyllie and Filson (1989) and averaged from four angles of incidence (0, 10, 20, and 30 degrees). The slightly nonlinear behavior of the stiff low-plasticity clays has been considered, and this amplification function was used to calculate UHFAS for return periods up to 475 years ($PGA_{T=475} \approx 200$ cm/sec^2 for rock sites, Table 1). Figure 9b compares UHS (5% damped) calculated using the proposed scheme (Fig. 1) for condition of hypothetical rock site and Leninakan, and Figure 9c shows normalized (divided by correspondent PGA value) UHS and standard curves dictated by the building codes for the territory of the former USSR and, therefore, for the Spitak region (Paz, 1994) for so-called average soil or soil category II; shallow (thickness of 15–20 m) clay in a hard state, or unsaturated sandy loam (ground water depth is more than 10 m).

It can be seen that the level of normalized UH spectra exceeds standard curve for periods longer than 0.4–0.5 Hz. It has been pointed out (Wyllie and Filson, 1989; Yegian *et al.*, 1994b) that the amounts of damage in Leninakan increased with the increase of the period of the structures, and 95% of residential buildings with periods more than 0.6 sec collapsed or had to be demolished due to heavy damage. At the same time, shorter-period (less than 0.4 sec) buildings in Leninakan were damaged approximately equally to those, for example, in Kirovakan, the other big city that experienced severe damage. As has been noted previously, following the building codes that were in force before the Spitak earthquake, seismic loads for Leninakan should be determined using the design curve for soil category II multiplied by design acceleration 200 cm/sec^2. Let us consider return period 475 years (10% probability of exceedance in 50 years) that is usually accepted for ordinary building. In this case, the design acceleration for Leninakan was estimated as 350 cm/sec^2 (see Table 1). It should be noted, that this value, as well as our estimations for rock site (200 cm/sec^2), coincides with calculations of peak horizontal accelerations on the rock outcrop and ground surface in Leninakan during the Spitak earthquake (250 cm/sec^2 and 320–390 cm/sec^2, respectively, after Yegian *et al.*, 1994c). Figure 9d shows comparison between the building code's response spectra (design curve multiplied by design accelerations 200 cm/sec^2, which was in force before the Spitak earthquake, and 400 cm/sec^2, which was stated after the earthquake) and UHS estimated for return period 475 years. Strong ground motion records from the main shock of the Spitak earthquake are not available for Leninakan. Yegian *et al.* (1994c) performed the 1-D soil-response analyses using characteristic soil profile models and adjusted main-shock accelerogram registered in town of Ghoukasian. The acceleration response spectra (N-S and E-W components) of calculated ground surface motion are also shown in Figure 9d. From the comparison, it is possible to conclude that the extensive building damage in Leninakan was caused not only by the effect of soil amplification, but also by the high overall level of seismic shaking as compared with the building code provisions which were in force before the earthquake. The uniform hazard site-dependent response spectrum estimated for return period 475 years almost completely overlaps the Spitak earthquake spectra (Fig. 9d), that suggests its applicability to be used in the building code. At the same time, new building code's

Table 1
Comparison of Ground-Motion Data and PGA Hazard Assessment Obtained Using Uniform Hazard Fourier Spectra

	PGA Hazard Assessment (cm/sec*sec) Return Period (years)						
Region and Site	50	100	200	475	1000	2000	PGA Values†
Northern Armenia							
Rock Site	50	85	130	200	280	360	200–250*
Leninakan City	70	110	170	350	—	—	320–390*
Western Uzbekistan							
Gazli Town	25	60	125	180	300	430	200–300‡

*The data from Yegian *et al.,* 1994c
†Observed during the earthquakes or were estimated independently.
‡The data from Shteinberg *et al.,* 1980

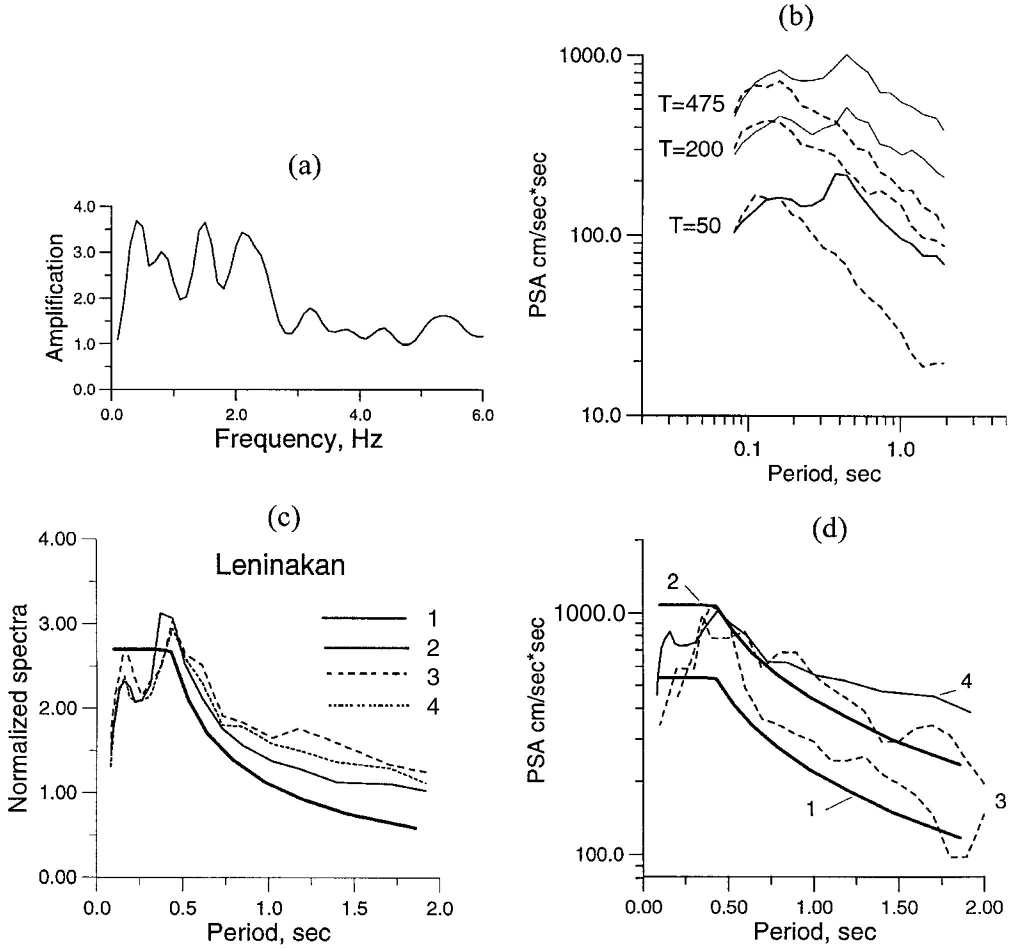

Figure 9. Leninakan city; (a) spectral amplification (soil/rock) for Leninakan city; (b) uniform hazard response spectra (5% damped) estimated for return periods T for condition of rock sites (dashed lines) and Leninakan city (solid lines); (c) comparison between the building code's standard "design" spectrum (1) and normalized uniform hazard response spectra estimated for return periods of 50 (2); 200 (3) and 2000 (4) years; (d) comparison of 5% damped response spectra for Leninakan city. 1, 2: spectra proposed by the building code ("design spectra" multiplied by "design acceleration") which were in force before the Spitak earthquake (1) and have been stated after the earthquake (2); 3: response spectra (N-S and E-W component) of estimated ground surface motion during the Spitak earthquake (Yegian *et al.,* 1994c); 4: uniform hazard response spectrum for return period of 475 years.

response spectrum seems to underestimate seismic loads for periods more than 1 sec. It is necessary to note that our assessment of seismic hazard has been obtained on the basis of tectonic and seismicity data that were available before the Spitak earthquake, although source scaling and attenuation model have been established on the basis of strong motion data obtained after the earthquake.

Actually, it is necessary to take into account the uncertainty of the duration estimated for a given "dominant earthquake". The influence of the duration variability may be estimated using calculations of the UH accelerograms assuming mean and mean $\pm$ standard deviation values. Fig. 10 shows UHS estimated for the conditions of rock site (the Spitak area) and deep deposits (the city of Leninakan) for return period of 475 years using mean, mean $-$ 1 σ, and mean $+$ 1 σ duration values for dominant earthquakes. The corresponding estimations of PGA values are listed in Table 2. The difference of the UHS estimations depends both on the accepted ground-motion duration values and oscillator period. Therefore, the uncertainty of the results causing by the ground-motion duration scatter should be estimated.

Figure 11a shows the UHS (5% damped) calculated for different return periods for the town of Gazli. Table 1 lists PGA values obtained from UHAs (average values from 40 simulations), and Figure 11b compares normalized (divided by correspondent PGA value) UHS and standard curves dictated by the building codes for the territory of the former USSR and, therefore, for the Gazli for soil category II. Fig-

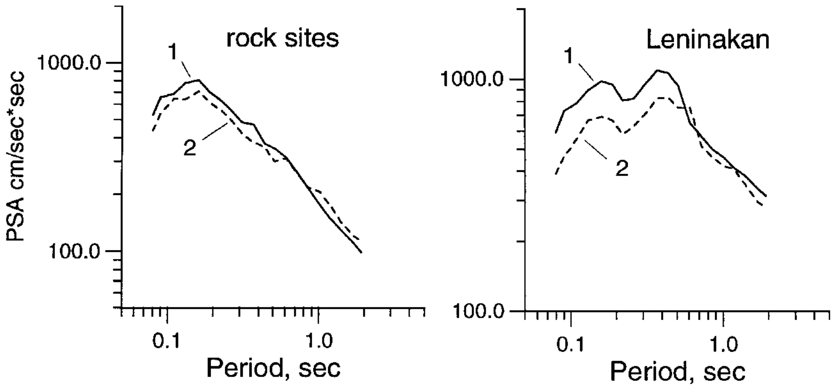

Figure 10. Uniform hazard response spectra (return period of 475 years, the Spitak region) estimated using different values of ground motion duration; 1: mean − standard deviation; 2: mean + standard deviation.

ure 11c shows comparison between the building code's response spectra (design curve multiplied by the design acceleration of 100 cm/sec^2, which was in force before 1976, and 200 cm/sec^2, which has been stated after the earthquake) and UH response spectra estimated for return periods of 475 and 1000 years. It is seen that, in this case, the shape of normalized UH response spectra depends on the chosen return period, and the ratio between long- and short-period spectral amplitudes decrease with increasing of return period. This phenomenon reflects the increase of relative contribution to spectral hazard at high frequencies from close events of $M = 6.0$ (that produce intensive high-frequency radiation) with increasing of return period. Peak ground acceleration values in the town of Gazli during the earthquakes of 1976 were estimated as about 200–300 cm/sec^2 (Shteinberg *et al.*, 1980), and our estimations are 180 cm/sec^2 and 300 cm/sec^2 for return periods of 475 and 1000 years, respectively (Table 1). It is seen from Figure 11c that the extensive building damage in the town of Gazli during the earthquakes of 1976 was caused by the high overall level of seismic shaking as compared with the building code provisions which were in force before the earthquakes. At the same time, results of seismic hazard calculation for return period of 1000 years, as well as existing "standard spectrum" for soil category II, may be considered as appropriate to be used as the code's provisions in this case.

Table 2
Peak Ground Acceleration (PGA) Estimations Obtained Using Different Duration Values for "Dominant Earthquakes"*

Magnitude	Duration Values (sec) mean − 1 st. dev.	mean	mean + 1 st. dev
	Spitak region, rock site		
5.0	2.8	4.5	7.0
6.0	4.6	7.2	11.0
7.0	8.0	11.5	18.0
	PGA, cm/sec*sec		
	250	200	180
	Leninakan city		
5.0	3.7	6.4	7.0
6.0	5.6	9.7	17.0
7.0	8.4	14.6	25.0
	PGA, cm/sec*sec		
	420	350	300

*Return period 475 years.

Conclusions

This article presents an integrated approach for evaluating site-dependent seismic hazard in terms of ground-motion parameters used for engineering purposes. In the proposed approach, a probabilistic seismic-hazard analysis in terms of Fourier acceleration spectra is performed to generate a hazard curve. The site-dependent uniform hazard Fourier spectra are obtained for a given soil condition using spectral amplification functions. Then, the so-called dominant earthquakes contributing to the hazard are determined for a given return period (probability of exceedance) in the considered frequency range. The uniform hazard Fourier spectra are weighted taking into account the contribution from dominant earthquakes to produce the so-called weighted spectra that represent the influence from dominant earthquakes. These weighted spectra combined with strong-motion duration determined for dominant earthquakes are used to generate ground-motion time series, the summation of which produce Uniform Hazard spectra-compatible accelerograms, or UHAs. The hazard-compatible site & region & return period-dependent PGA and response spectra (uniform hazard response spectra) are determined using these time functions which, in turn, may be used as design ground motion for dynamic analyses of structures. The approach has been tested by using for estimation of design parameters (response spectra and PGAs) for regions recently experiencing destructive earthquakes, namely, northern Armenia, the Lesser Caucasus (region of the Spitak earthquake of 1988), and Gazli, Central Asia (region of the Gazli earthquakes of 1976 and 1984). The estimations of "site & region-dependent" PGA and response spectra for the return periods of 475 and 1000 years (10% and 5% probability of exceedance in 50 years), that were obtained using the proposed approach, were compared with the data observed (or estimated independently) during these earthquakes.

The major goal of every seismic-hazard map is to pro-

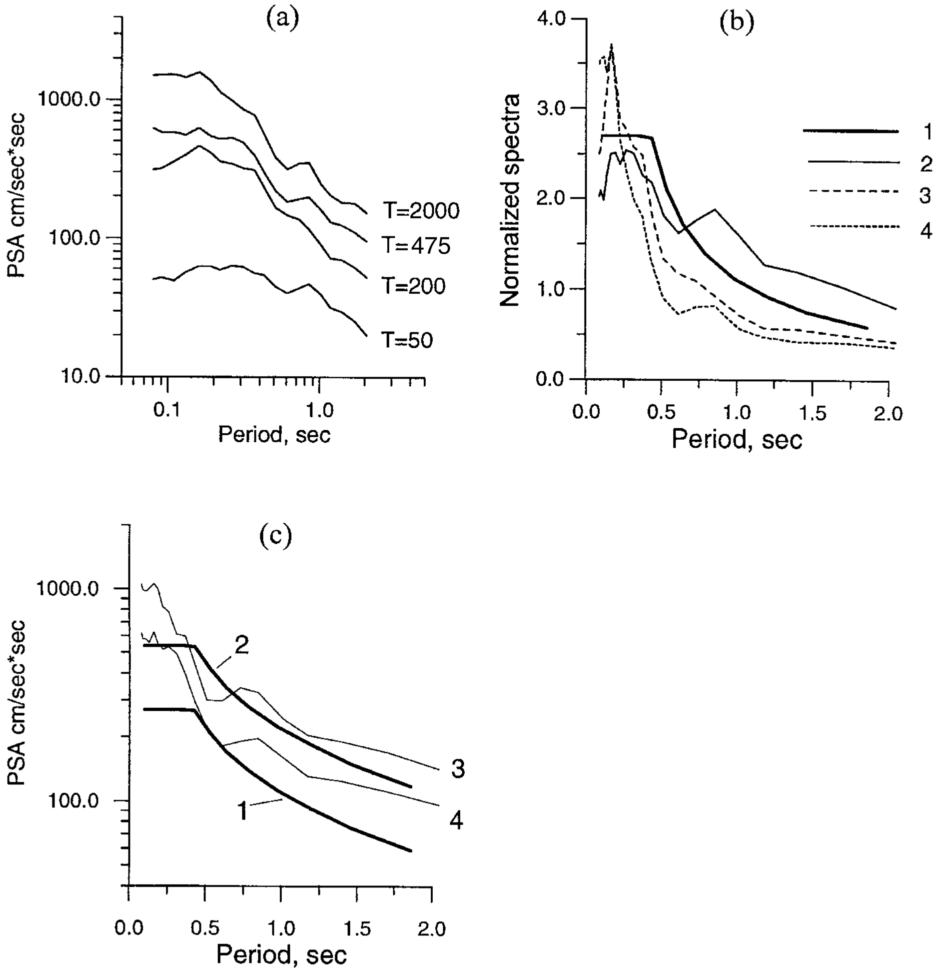

Figure 11. The town of Gazli; (a) uniform hazard response spectra (5% damped) estimated for various return periods *T*; (b) comparison between the building code's standard "design" spectrum (1) and normalized uniform hazard response spectra estimated for return periods of 50 (2); 200 (3) and 2000 (4) years; (c) comparison of 5% damped response spectra for the town of Gazli. 1, 2: spectra proposed by the building codes ("design spectra" multiplied by "design acceleration") which were in force before the Gazli earthquakes of 1976 (1) and have been stated after the earthquakes (2); 3, 4: uniform hazard response spectra for return period of 475 and 1000 years, respectively.

vide an information on the expected seismic influence, and the engineers should design the construction to be able to withstand the level of vibration. Thus, a question arises "are these hazard estimations reliable, or how do you (a seismologist) propose to test your predictions?". Obviously, the best test is the comparison of actual strong earthquake effects and hazard maps. So long as the recent building code requirements are based on the results of probabilistic seismic-hazard assessment, every strong earthquake provides an unique opportunity to verify the seismic-hazard-assessment technique, as well as the general principles of design parameters [seismic zone factor (PGA), response spectra shapes, etc.] adoption. Obviously, the provisions should be, at least, roughly consistent with the future earthquake influence. In the considered cases, the results of the technique application show an agreement with the observed effect. Of course, it is only one realization of an earthquake ground motion, but it is the largest observed one, and it is seen that the proposed technique is able to predict the level of the vibration. This suggests that these estimations may be used as a reliable basis for building code provisions and engineering decisions, and bearing in mind reasonable conservatism the recommended hazard level for conventional buildings should correspond to a return period of 1000 years (a probability of 0.05 within 50 years) at least for the considered regions. The scheme can also be used as a basis for probabilistic ("return period-dependent") microzonation in terms of engineering ground-motion parameters.

The proposed approach allows to obtain, simultaneously, during a single computational running, the "site & region-dependent" design ground-motion parameters, which are used in engineering practice (PGA, response spectra with various damping ratios, capacity spectra, time histories), using a common ground-motion models. Seismic-hazard assessment in terms of macroseismic intensity (MSK or MMI scales) can also be obtained using recently established relationships between intensity values and the Fourier amplitude spectra (Sokolov and Chernov, 1998).

The author realizes that there are some simplified assumptions both in the input data and calculation scheme. For example, the Poisson-process model was used to describe the earthquake occurrence; a simple point-source ω-squared model was used for calculation of spectral amplitudes near the extended source; linear model of soil response has been used for weak and strong, distant and close events; generalized envelope function was used in ground-motion generation, and so forth. However, the general scheme of the approach is capable of being improved as new and more complete data appear.

Acknowledgments

The author is very grateful to Ivan Wong, Mark Petersen and an anonymous reviewer for their constructive suggestions and comments that allow the author to improve the manuscript.

References

Abrahamson, N. A., and K. M. Shedlock (1997). Overview, *Seism. Res. Lett.* **68,** 9–23.

Atkinson, G. M. (1993). Earthquake source spectra in Eastern North America, *Bull. Seism. Soc. Am.* **83,** 587–596.

Atkinson, G. M., and R. F. Mereu (1992). The shape of ground motion attenuation curves in southeastern Canada, *Bull. Seism. Soc. Am.* **82,** 2014–2031.

Atkinson, G. M., and D. M. Boore (1995). Ground-motion relations for eastern North America, *Bull. Seism. Soc. Am.* **85,** 17–30.

Atkinson, G. M., and W. Silva (1997). An empirical study of earthquake source spectra for California earthquakes, *Bull. Seism. Soc. Am.* **87,** 97–113.

Bard, P. Y. (1995). Effects of surface geology on ground motion: recent results and remaining issues, *Proceedings of 10th European Conference on Earthquake Engineering,* Balkema, Rotterdam, 305–323.

Bazzuro, P., and C. A. Cornell (1998). Disaggregation of seismic hazard, *Bull. Seism. Soc. Am.* **89,** 501–520.

Bereznev, I. A., and G. M. Atkinson (1997). Modeling finite-fault radiation from ω^n spectrum, *Bull. Seism. Soc. Am.* **87,** 67–84.

Boatwright, J., and G. Choy (1992). Acceleration source spectra anticipated for large earthquakes in northeastern North America, *Bull. Seism. Soc. Am.* **82,** 660–680.

Bommer, J. J., A. S. Elnashai, G. O. Chlimimtzas, and D. Lee (1998). Review and development of response spectra for displacement-based seismic design, ESEE Research Report, 98-3, Imperial College, London, 163 pp.

Boore, D. M. (1983). Stochastic simulation of high frequency ground motion based on seismological model of the radiated spectra, *Bull. Seism. Soc. Am.* **73,** 1865–1894.

Boore, D. M. (1987). The prediction of strong ground motion, in *Strong Ground Motion Seismology,* M. Erdic and M. N. Toksoz (Editors), D. Reidel, Dordrecht.

Boore, D. M., and G. M. Atkinson (1987). Stochastic prediction of ground motions and spectral response parameters at hard-rock sites in eastern North America, *Bull. Seism. Soc. Am.* **77,** 440–467.

Borcherdt, R. D. (1994). Estimates of site-dependent response spectra for design (methodology and justification), *Earthquake Spectra* **10** no. 4, 617–653.

Brune, J. N. (1970). Tectonic stress and the spectra of seismic shear waves from the earthquakes, *J. Geophys. Res.* **75,** 4997–5009.

Caillot, V., and P.-Y. Bard (1992). Band limited duration and spectral energy: empirical dependence on frequency, magnitude, hypocentral distance and site conditions, in *Proceedings of 10th World Conference on Earthquake Engineering,* Balkema, Rotterdam, 781–786.

Campbell, K. W., and Y. Bozorgnia (1994). Near-source attenuation of peak horizontal acceleration from Northridge accelerogram recorded from 1957 to 1993, *Proceedings of 5th US National Conference on Earthquake Engineering,* Chicago.

Cao, T., M. D. Petersen, C. H. Cramer, T. R. Toppozada, M. S. Reichle, and J. F. Davis (1999). The calculation of expected loss using probabilistic seismic hazard, *Bull. Seism. Soc. Am.* **89,** 867–876.

Chernov, Yu. K. (1989). Strong Ground Motion and Quantitative Assessment of Seismic Hazard, Tashkent, Fan Publishing House (in Russian).

Chernov, Yu. K., and V. Yu. Sokolov (1991). Quantitative estimation of probable seismic effect for northeastern part of Sakhalin island, Yuzhno-Sakhalinsk, Institute of Marine Geology and Geophysics (in Russian).

Coppersmith, K. J. (1991). Seismic source characterization for engineering seismic hazard analyses, in *Proceeding of the Fourth International Conference on Seismic Zonation,* Stanford, California, August 25–29, 1991, vol. **I,** 3–60.

Cornell, C. A. (1968). Engineering seismic risk analysis, *Bull. Seism. Soc. Am.* **58,** 1583–1606.

Denham, D., and W. Smith (1993). Earthquake hazard assessment in the Australian Southwest Pacific Region: a review of the status quo, *Annali di Geofisica* **XXXVI,** no. 3–4, 27–39.

Dowrick, D. J., K. R. Berryman, G. H. McVerry, and J. Z. Zhao (1998). Earthquake hazard in Christchurch, *Bull. New Zealand Nat. Soc. Earthquake Eng.* **31,** 1–23.

Djuraev A., I. A. Ershov, E. V. Popova, and N. V. Shebalin (1986). Macroseismic observation of territory of town of Gazli after the earthquake of 19(20) March 1984, in *Detailed Engineering-Seismological Research* (Engineering Seismology Problems, Issue 27), Moscow, Nauka Publishing House (in Russian).

EERI (1989). The basics of seismic risk analysis, *Earthquake Spectra* **5,** 675–702.

Esteva, L. (1988). The Mexico earthquake of September 19, 1985: consequences, lessons and impact on research and practice, *Earthquake Spectra* **4,** 413–426.

FEMA (1999). Earthquake loss estimation methodology, HAZUS99, Technical manual.

Field, E. H., and K. H. Jacob (1995). A comparison and test of various site-response estimation techniques, including three that are not reference-site dependent, *Bull. Seism. Soc. Am.* **85,** 1127–1143.

Harmsen S., D. Perkins, and A. Frankel (1999). Deaggregation of probabilistic ground motions in the central and eastern United States, *Bull. Seism. Soc. Am.* **89,** 1–13.

Huo, J.-R., and Y. Hu (1994). Magnitude and distance dependent envelope function of acceleration time history, in *Proceedings of Fifth U.S. National Conference on Earthquake Engineering,* Chicago, 10–14 July 1994, Vol. III, 168–178.

Ibragimov, R. N. (1989). Identification of seismogenic zones on territory of western Uzbekistan, *Uzbek Geol. J.* **3,** 11–15 (in Russian).

Irikura K., T. Iwata, H. Sekiguchi, A. Pitarka, and K. Kamae (1996). Lessons from the 1995 Hyogo-Ken Nanbu earthquake: why where such destructive motions generated to buildings? *J. Nat. Disaster Sci.* **17,** 99–127.

Jacob, K. H. (1991). Seismic zonation and site response: are building-code soil-factors adequate to account for variability of site conditions across the US? in *Proceedings of Fourth International Conference on Seismic Zonation,* Stanford, California, 695–702.

Jakob, K., J. Armbruster, N. Barstow, and S. Norton (1994). Probabilistic ground motion estimates for for New York: comparison with design ground motions in national and local codes, in *Proceeding of the Fifth U.S. National Conference on Earthquake Engineering,* Chicago, 10–14 July 1994, Vol. III, 119–128.

Joyner, W. B., and D. M. Boore (1986). On simulating large earthquakes by Green's function addition of smaller earthquakes, in *Proceedings of the Fifth Maurice Ewing Symposium on Earthquake Source Mechanics,* S. Das, J. Boatwright, and C. Scholz (Editors). American Geophysical Union, 269–274.

Krawinkler, H. (1995). New trends in seismic design methodology, in *Proc. 10th European Conf. on Earthquake Engineering,* Balkema, Rotterdam, 821–830.

Krestnikov, V. N., T. P. Belousov, and D. V. Shtange (1980) Seismotectonic conditions of the occurrence of the Gazli earthquakes of 1976, *Bull. (Izv.) Acad. Sci. USSR, Earth Physics* **16,** 648–660.

Little, T. E., and K. M. Meidal (1994). Ground motion studies for a West Coast electric utility, in *Proceedings of the Fifth U.S. National Conference on Earthquake Engineering,* Chicago, 10–14 July 1994, Vol. III, 261–270.

Mahdavian, A., and T. Sasatani (1994). Predictive modeling of earthquake ground motion in the northern part of Japan, in *Proceedings of the Fifth U.S. National Conference on Earthquake Engineering,* Chicago, 10–14 July 1994, Vol. III, 231–240.

Masopust, R. (1999). Seismic resistance experience in application to equipment of critical facilities, in *Proceedings of the Eleventh European Conference on Earthquake Engineering,* P. Bilsh, P. Labbe, and A. Pecker (Editors), Balkema, Rotterdam, 119–130.

McGuire, R. K. (1995). Probabilistic seismic hazard analysis and design earthquakes: closing the loop, *Bull. Seism. Soc. Am.* **85,** 1275–1284.

Medvedev, S. V. (Editor) (1976). Seismic Zoning of the USSR, trans. by U.S. Department of Commerce.

Newmark, N. M., and W. J. Hall (1973). Procedures and criteria for earthquake resistant design: building practices for disaster mitigation, National Bureau of Standards, *Building Science Services* **46,** no 1, 209–237.

Paz, M. (Editor) (1994). International Handbook of Earthquake Engineering: Codes, Programs, and Examples, Chapman & Hall, New York.

Petersen, M. D., K. H. Jacob, L. R. Sykes, and J. Pacheco (1991). Regional probabilistic seismic hazard analysis for the San Francisco Bay area in *Proceedings of Fourth International Conference on Seismic Zonation,* Stanford, California, 707–714.

Petersen, M. D., W. A. Bryant, C. H. Cramer, M. S. Reichle, and C. R. Real (1997). Seismic ground-motion hazard mapping incorporating site effects for Los Angeles, Orange, and Ventura counties, California: a geographical information system application, *Bull. Seism. Soc. Am.* **87,** 249–255.

Pletnev, K. G., N. V. Shebalin, and V. V. Shteinberg (1977). Strong-motion records from the May 1976 Gazli USSR earthquakes, *U.S. Geol. Surv. Circular 762A,* 3–5.

Rovelli, A., O. Bonamassa, M. Cocco, M. Di Bona, and S. Mazza (1988). Scaling laws and spectral parameters of the ground motion in active extensional areas in Italy, *Bull. Seism. Soc. Am.* **78,** 550–560.

Schenk, V., Z. Schenkova, and P. Kottnauer (1996). Earthquake hazard assessment for the Czech republic and adjacent area, in *Earthquake Hazard and Risk,* V. Schenk (Editor), Kluwer, Netherlands, 125–140.

Semenov, R. M., V. Yu. Kharakhinov, and V. A. Pavlenov (1996). The large North Sakhalin earthquake of May 28, 1995: a seismological description, *Izvestiya, Physics Solid Earth* **12,** 124–129 (in Russian).

Shan, H., R. Boyle, and W. Dong (1991). Geographic information systems and artificial intelligence: an application for seismic zonation, in *Proceeding of the Fourth International Conference on Seismic Zonation,* Stanford, California 25–29 August 1991, Vol. I, 487–517.

Shapira, A., and T. Van Eck (1993). Synthetic uniform-hazard site specific response spectrum, *Natural Hazards* **8,** 201–215.

Shin, T. C., K. W. Kuo, W. H. K. Lee, T. L. Teng, and Y. B. Tsai (2000). A preliminary report on the 1999 Chi-Chi (Taiwan) earthquake, *Seism. Res. Lett.* **71,** 24–30.

Shteinberg, V. V., I. G. Ivanova, and V. M. Grayzer (1980). The earthquake in Gazli on May 17, 1976, *Bull. (Izv.) Acad. Sci. USSR, Earth Physics* **16,** 159–167 (in Russian).

Shteinberg, V. V. (1983). On the earthquake source parameters and seismic effect during the earthquakes, *Izvestiya, Physics of the Solid Earth* **7,** 49–64 (in Russian).

Shteinberg, V. V. (1986). Ground motion parameters during strong earthquakes, in *Detailed Engineering-Seismological Research* (Engineering Seismology Problems, issue 27), Moscow: Nauka Publishing House (in Russian).

Sikharulidze, D. T., N. T. Tutberidze, A. Kh. Bagramyan, P. D. Dzhidzheishvili, B. Ts. Yeremyan, N. A. Nibladze, M. E. Tamazashvili, and R. D. Shavishvili (1983). Structure, Tense-Deformed State and Seismic Conditions of the Lithosphere of the Minor Caucasus, Tiflis, Metznirieba Publishing House, (in Russian).

Sokolov, V. Yu. (1998a). Spectral parameters of the ground motions in Caucasian seismogenic zones, *Bull. Seism. Soc. Am.* **88,** 1338–1444.

Sokolov, V. Yu. (1998b). Rough estimation of site response using earthquake ground motion records, in *Proceedings of the Second International Symposium on the Effects of Surface Geology on Seismic Motion,* Yokohama, Japan, 1–3 December, 1998, Balkema, Rotterdam, 517–522.

Sokolov, V. Yu. (1998c). Ground acceleration spectra from Caucasus earthquakes, *Izvestiya, Physics Solid Earth* **34,** 663–675.

Sokolov, V. Yu, and Yu. K. Chernov (1998). On the correlation of seismic intensity with Fourier amplitude spectra, *Earthquake Spectra* **14,** 679–694.

Sokolov, V. Yu., C.-H. Loh, and K.-L. Wen (2000). Empirical model for estimating Fourier amplitude spectra of ground acceleration in Taiwan region, *Earthquake Eng. Structural Dyn.* **29,** 339–357.

Somerville, P. (1998). Ground motion attenuation relationships and their application to aseismic design and seismic zonation, in *Proceedings of the Second International Symposium on the Effects of Surface Geology on Seismic Motion,* Yokohama, Japan, 1–3 December 1998, Balkema, Rotterdam, 35–49.

Toki, K., T. Sato, and J. Kiyono (1991). Estimation of peak acceleration for seismic microzonation taking into account the fault extent, in *Proceedings of Fourth International Conference on Seismic Zonation,* Stanford, California, 731–738.

Trifunac, M. D. (1990). A microzonation method based on uniform risk spectra, *Soil Dyn. Earthquake Eng.* **9,** 34–43.

Trifunac, M. D., and V. W. Lee (1989). Empirical model for scaling Fourier amplitude spectra of strong ground acceleration in terms of magnitude, distance, site intensity and recording site conditions, *Soil Dyn. Earthquake Eng.* **8,** 110–125.

Trifunac, M. D., and E. I. Novikova (1995). State of art review on strong motion duration, in *Proceedings of 10th European Conference on Earthquake Engineering,* Balkema, Rotterdam, 131–140.

Wyllie, L. A., and J. R. Filson (1989). Armenia earthquake reconnaissance report, *Earthquake Spectra* (special supplement).

Yegian, M. K., V. G. Ghahraman, and G. Gazetas (1994a). 1988 Armenia earthquake. I: Seismological, geotechnical and structural overview, *J. Geotech. Eng.* **120,** 1–20.

Yegian, M. K., V. G. Ghahraman, and G. Gazetas (1994b). 1988 Armenia earthquake. II: Damage statistics versus geologic and soil profiles, *J. Geotech. Eng.* **120,** 21–45.

Yegian, M. K., V. G. Ghahraman, and G. Gazetas (1994c). Ground motion and soil response analyses for Leninakan, 1988 Armenia Earthquake, *J. Geotech. Eng.* **120,** 330–348.

Youngs, R. R., N. Abrahamson, F. I. Makdisi, and K. Sadigh (1995). Magnitude-dependent variance of peak ground acceleration, *Bull. Seism. Soc. Am.* **85,** 1161–1176.

Zerva, A., A. P. Petropulu, and P.-Y. Bard (1999). Blind deconvolution for site-response evaluation exclusively from ground-surface seismic recordings, *Soil Dyn. Earthquake Eng.* **18,** 47–57.

Geophysical Institute
Karlsruhe University
Herzstrasse 16
Karlsruhe 76187, Germany
Vladimir.Sokolov@gpi.uni-karlsruhe.de

Manuscript received 29 July 1999.